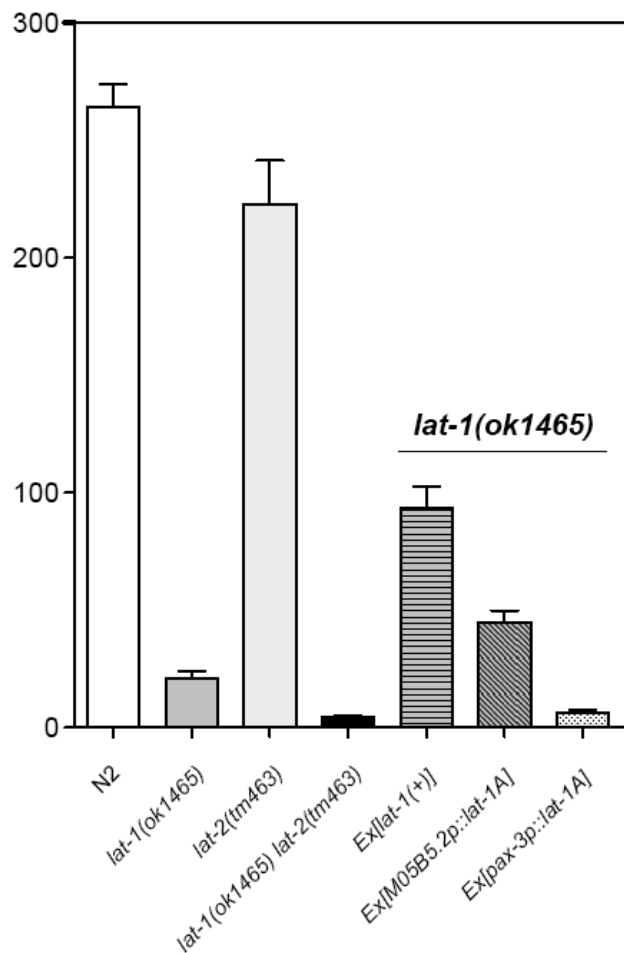## Supplemental Data

Latrophilin Signaling Links Anterior-Posterior

Tissue Polarity and Oriented Cell Divisions
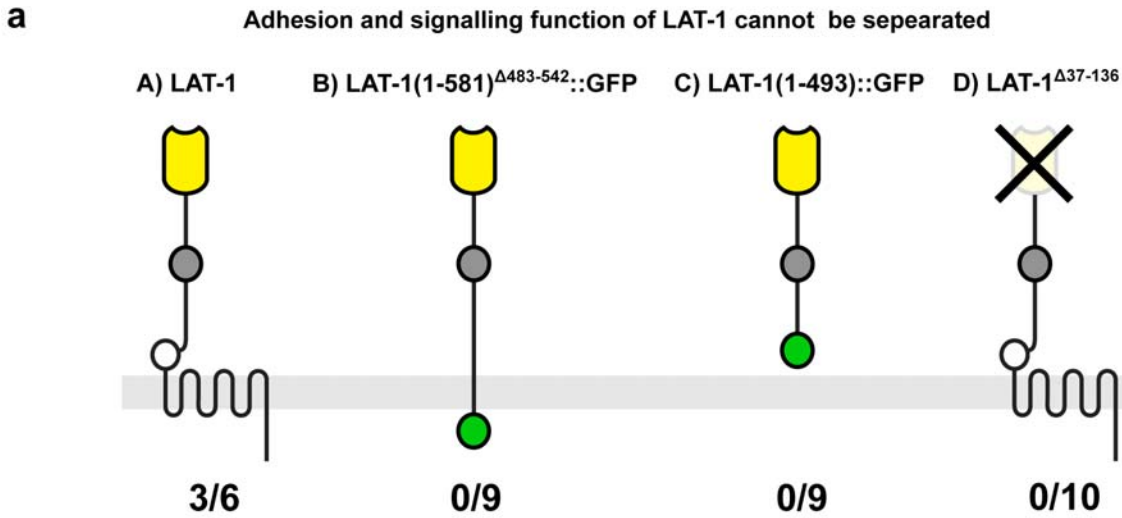
in the *C. elegans* Embryo

Tobias Langenhan, Simone Prömel, Lamia Mestek, Behrooz Esmaeili, Helen Waller-Evans, Christian Hennig, Yuji Kohara, Leon Avery, Ioannis Vakonakis, Ralf Schnabel, and Andreas P. Russ
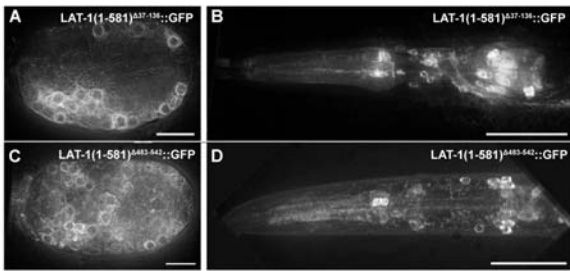

Figure S1.
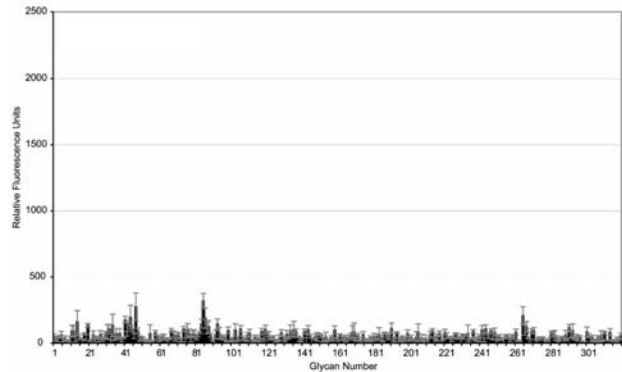Number of adult offspring for latrophilin mutants and transgenic hermaphrodites carrying different lat-1 constructs. Due to random loss of transgenic arrays the efficiency of rescue for the complementing transgene *Ex[lat-1(+)]* is only expected to be ~50% of the wild type brood size. Note that the transgene active in epidermal precursors (*pax-3p::lat-1A*) actually reduces brood size (confirmed with several independent arrays).

a Adhesion and signalling function of LAT-1 cannot be seperated

A) LAT-1   B) LAT-1(1-581)$^{\Delta 483-542}$::GFP   C) LAT-1(1-493)::GFP   D) LAT-1$^{\Delta 37-136}$

3/6   0/9   0/9   0/10

b LAT-1$^{\Delta 37-136}$ and LAT-1$^{\Delta 483-542}$ expression patterns

A LAT-1(1-581)$^{\Delta 37-136}$::GFP   B LAT-1(1-581)$^{\Delta 37-136}$::GFP

C LAT-1(1-581)$^{\Delta 483-542}$::GFP   D LAT-1(1-581)$^{\Delta 483-542}$::GFP

c *C. elegans* RBL domain does not bind glycans

d RBL(D45E) enables L-rhamnose binding of LAT-1

C. elegans RBL domain   *C. elegans* RBL domain D45E
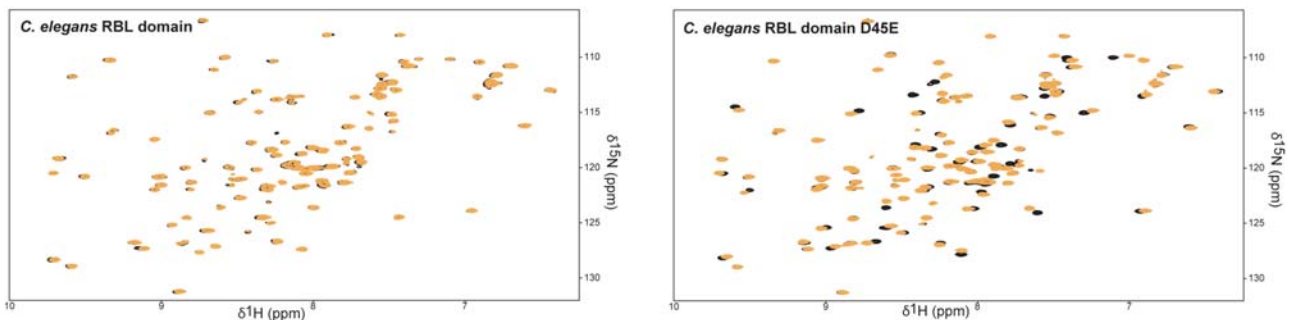
Figure S2.

RBL proteins were initially isolated from sea urchin eggs by their lectin activity (Ozeki et al., 1991a; Ozeki et al., 1991b). We recently described the structure of the RBL domain of the murine latrophilin LPHN1, and found it to have only very weak carbohydrate-binding properties (Vakonakis et al., 2008). We also noted that a residue critical for carbohydrate binding in murine LPHN1 is substituted in *C. elegans* LAT-1 (Asp45), and predicted that LAT-1 would be completely devoid of carbohydrate-binding activity.

As the physiological ligands of latrophilins are unknown, we tested the molecular requirements for LAT-1 signalling *in vivo* using a transgenic rescue assay. No complementation of the *lat-1(ok1465)* mutant phenotype was observed with a construct lacking the RBL domain (LAT-1$^{\Delta 37-136}$) but retaining the hormone-binding (HRM), GPS, and 7TM domains (Fig. S2a) (Steinel and Whitington, 2009).

This indicates that the rescuing activity of *lat-1* transgenes is absolutely dependent on the presence of the RBL domain.

A N-terminal fragment of LAT-1 containing an RBL and stalk domain tethered to a single transmembrane region was inactive (LAT-1(1-581)$^{\Delta483-542}$::GFP, Fig. S2a), suggesting that the N-terminal region does not act as a passive adhesive anchor or as a membrane-bound ligand for a signal-transducing counter-receptor on a neighbouring cell. Similarly, a construct expressing a non-tethered N-terminal fragment resembling the N-terminal fragment that might be secreted or "shed" from LAT-1 expressing cells after GPS cleavage (Volynski et al., 2004) was inactive in our transgenic rescue assay (LAT-1(1-493)::GFP, Fig. S2a). Thus, we have not been able to functionally separate the putative adhesion and signal-transducing domains of *lat-1*, and did not find evidence for non-cell autonomous activity.

We investigated carbohydrate binding to the recombinant LAT-1 RBL domain. NMR spectra of this domain under physiological conditions show an appropriately folded protein (Fig. S2d). The crosspeaks of hydrogen and nitrogen frequencies would be expected to shift upon ligand binding, as seen in the murine LPHN1 RBL domain (Vakonakis et al., 2008). We did not observe such shifts upon addition of L-rhamnose even at high concentrations (Fig. S2d), indicating lack of rhamnose binding. The same was the case for addition of D-galactose, D-fucose, glucose, mannose, D-glucuronic acid, N-acetylgalactosamine, N-acetylglucosamine and heparin. The conservative substitution D45E restored the rhamnose binding activity of the recombinant LAT-1 RBL domain, further validating our prediction (Fig. S2d) (Vakonakis et al., 2008). An extended screen of 320 immobilized mono- to tetra-saccharides targets did not show glycan binding for the *lat-1* RBL domain (Fig. S2c). These results strongly suggest that while the conserved RBL domain is absolutely required for LAT-1 function *in vivo*, it does not act as a typical lectin binding to a common carbohydrate ligand.

(a) Domain requirements for LAT-1 function. Transgenic rescue of the *lat-1(ok1465)* phenotype was assayed with construct expressing different variants of LAT-1. Numbers below the sketches represent the number of independently rescued transgenic strains relative to all transgenic lines generated with a given construct.

The phenotype could only be complemented with the wild type receptor (A) but not with a membrane-anchored (B) or secreted (C) N-terminal domain, or with a full length receptor lacking only the RBL domain (D).

(b) Removing the RBL domain does not change localization of a membrane-anchored LAT-1-GFP fusion protein. Scale bars = 10 μm.

(c) *C. elegans* RBL domain does not show specific binding in glycan array assay.

(d) The RBL(D45E) modification enables rhamnose binding of LAT-1 RBL.
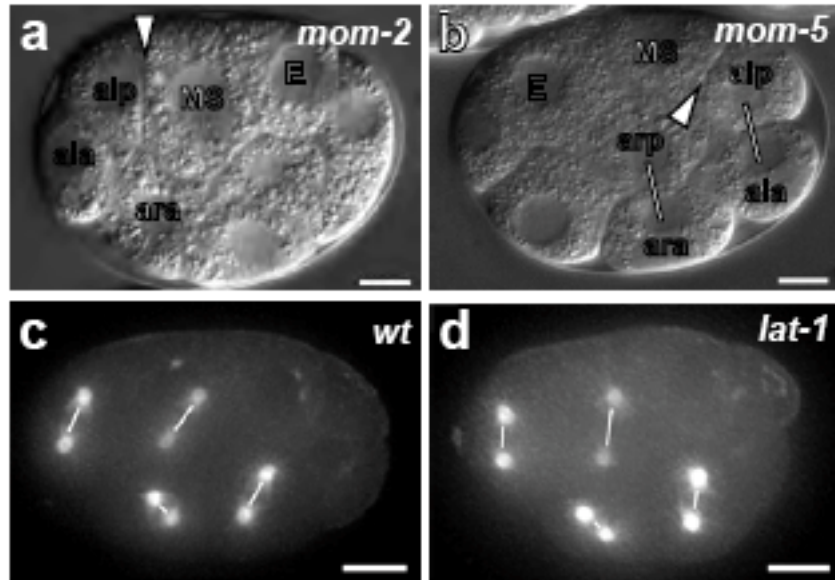
Figure S3.

(a and b) *mom-2(or42)* (e) and *mom-5(zu193)* (f) mutant embryos display normal contact of MS and ABalp (white arrowheads) and anterior position of ABala. Lack of *mom-2/mom-5* signaling results in a changed division axis of ABar (white bars), which assumes an orientation parallel to ABal, ABpl and ABpr.

(c and d) AB^4 division planes of *lat-1* embryos (d) are similar to wild type control (c) with ABar spindle orientation perpendicular to the other ABxx spindles.

In all embryos except (b) anterior is to the left, posterior to the right, ventral (MS) up. To visualize the ABar axis defect the embryo in (b) anterior is to the right, posterior to the left.

Embryos in c, d provide the starting time point for panels Figure 3 e-l.
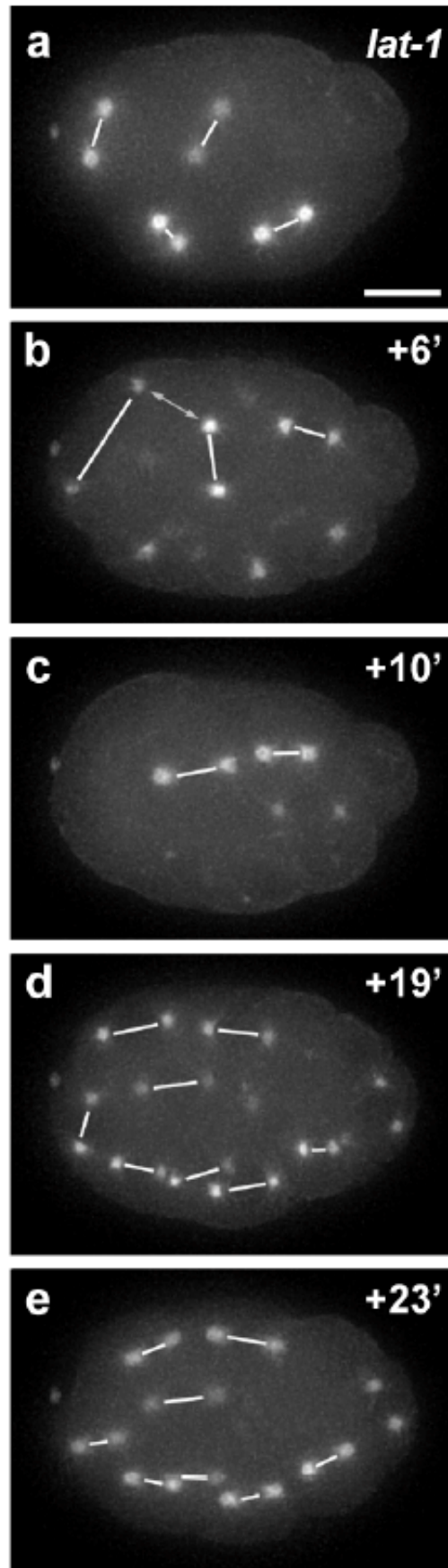
Figure S4.
Additional *lat-1* embryo, recording and annotation as in Fig. 3.
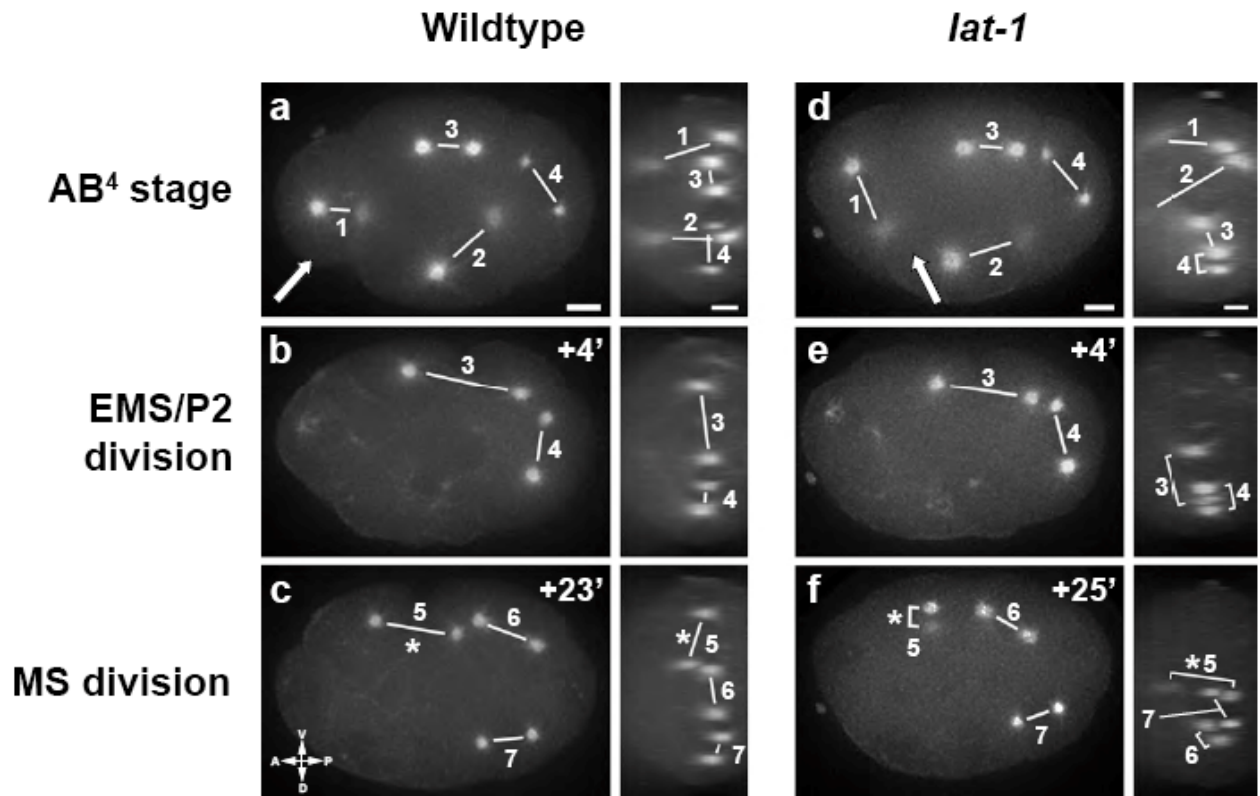
Figure S5.

Mitotic spindle alignment defects in latrophilin mutants visualized by β-tubulin::GFP. Centromere pairs are linked by white line. 1 = ABa, 2 = ABp, 3 = EMS, 4 = P_1, 5 = MS, 6 = E, 7 = C.

White arrows in left panels of (a) and (d) indicate the angles from which the corresponding Z-stack in the right panel is viewed. The Z-stack clearly visualizes division plane orientation into the plane of view that are hard to see in the standard panels. Note that ABa and ABp divide normally into the plane of view, as does MS in the *lat-1* mutant in (f).

All embryos are depicted in anterior to the left, ventral up. Scale bars = 5 μm.
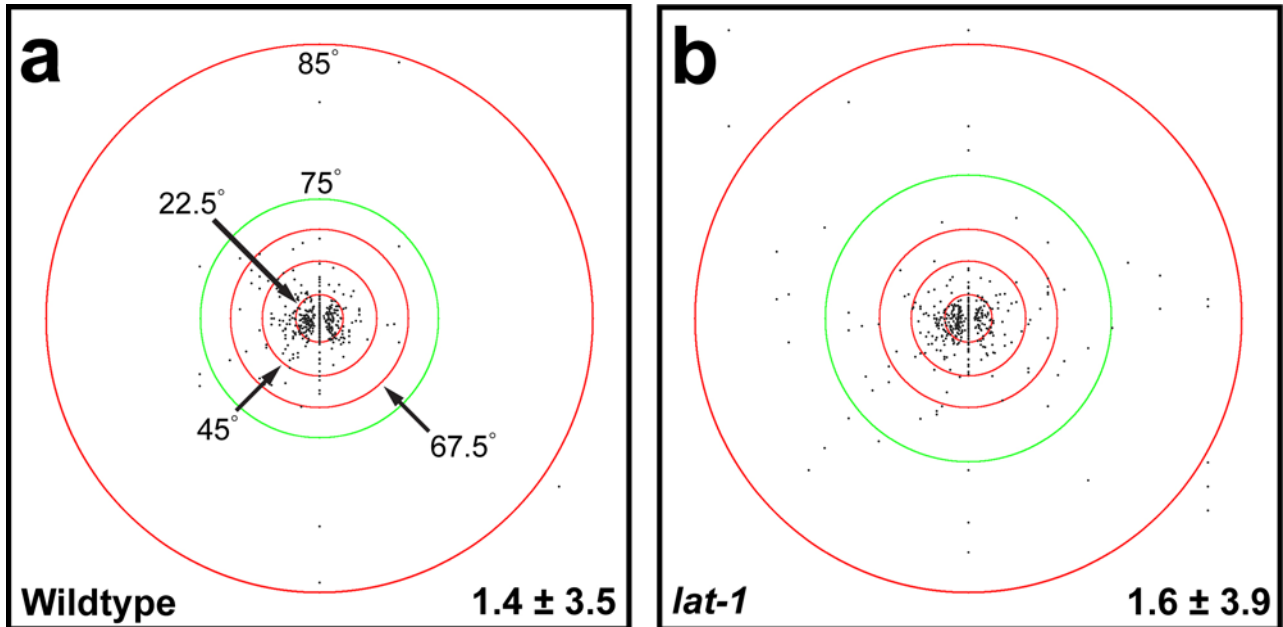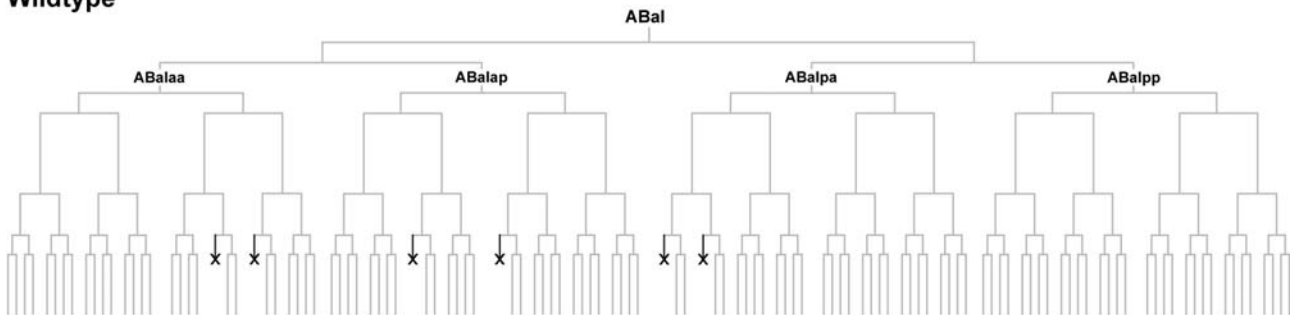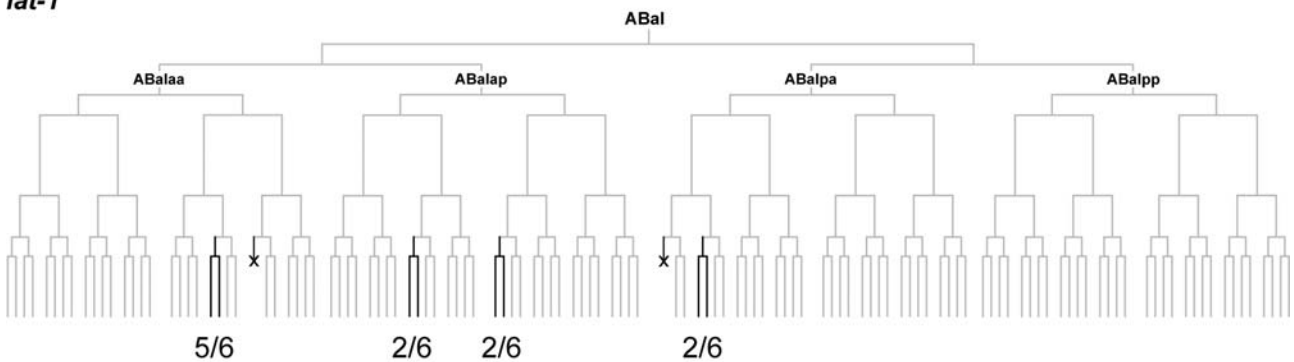
Figure S6.

Cell positioning defects in latrophilin mutants.

(a and b) Löwe projections of a wild type (a) and a *lat-1* embryo (b) demonstrate that sporadic defects in a-p division plane alignment occur in latrophilin mutant embryos. Dots close to the center represent cells dividing in a-p direction, increasing distance from the center represents increasing deviation from ideal a-p axis (for full explanation of Löwe projections see Bischoff and Schnabel, 2006).
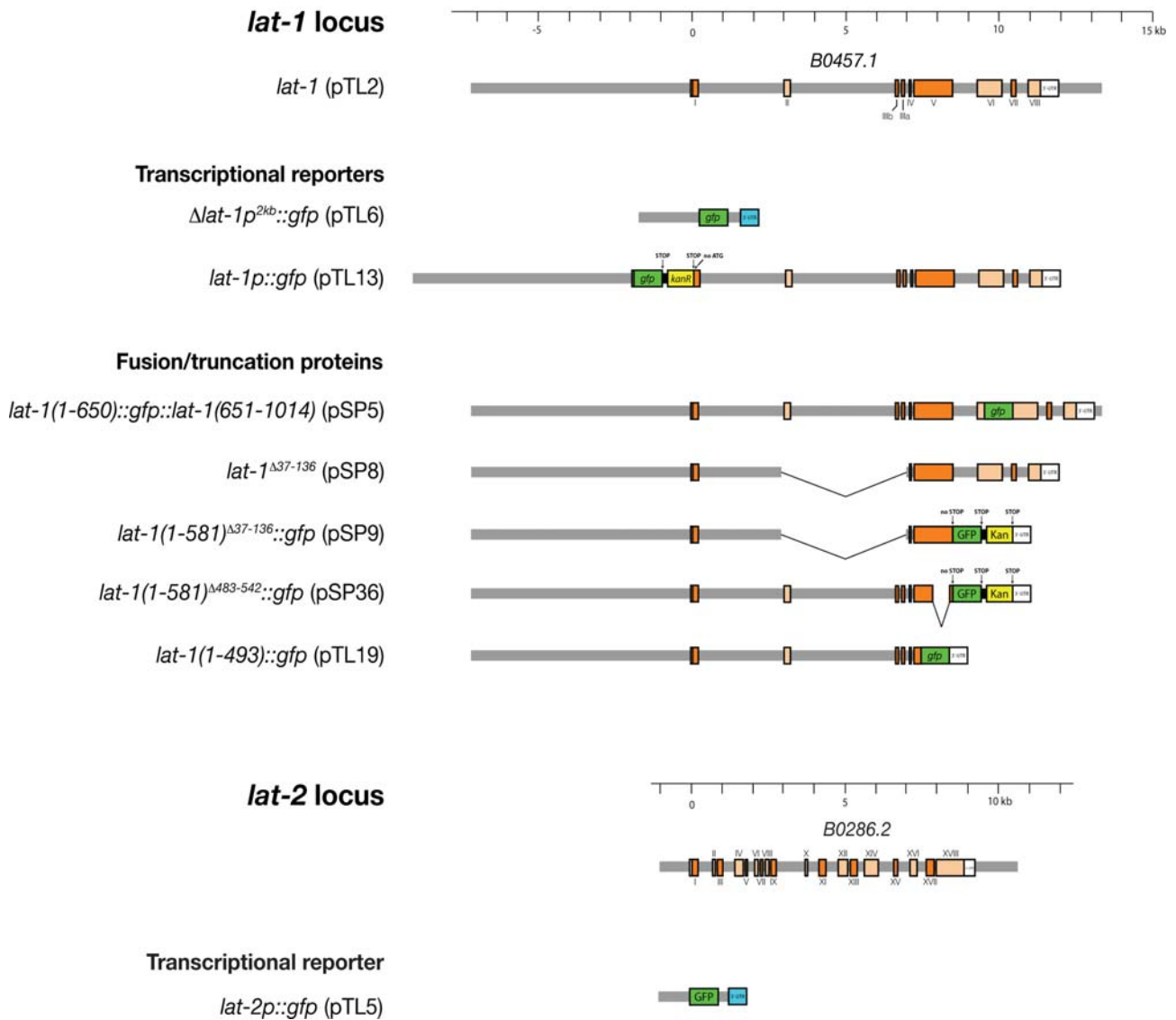

Figure S7.

The wild-type ABal lineage 6 early cell programmed cell deaths are observed (upper panel). In *lat-1* mutant embryos some of these cell deaths are absent (lower panel). Figures below sub-lineages indicate the number of embryos lacking cell death event over number of analyzed embryos.

Figure S8.

Transgene design for constructs used in the study. Most of the large transgenes are based on genomic cosmid clones and were generated by recombineering technology.

SUPPLEMENTAL EXPERIMENTAL PROCEDURES

Transgenes generated by cloning

Standard techniques were used to generate some constructs (see also Fig. S4). Transcriptional reporters were generated by amplifying a 2.0 kb region for *lat-1* (pTL6) and 1.0 kb for *lat-2* (pTL5) 5' of the ATG from genomic DNA, and inserted into pPD95.75. A 3.7 kb fragment including the entire coding region and 3'-UTR of *lat-1A* was PCR-amplified from EST clone *yk1336f09* with primers containing restriction sites *Kpn*I/*Bgl*II and inserted into pPD96.48. Promoter regions for heterologous expression (*M05B5.2* [1.0 kb]; *pax-3* [2.7 kb]) were PCR-amplified from N2 genomic DNA (for pTL24 and pSP14, respectively), *hsp16-41* promoter sequence was released by restriction digest from pPD49.83 (pTL37), and inserted into the *lat-1* cDNA plasmid (pPD49.83, pPD95.75 and pPD96.48 are gifts from Andy Fire). To construct a suitable *lat-1*-only cosmid, loci flanking the *lat-1* locus from cosmid *B0457* cosmid DNA was double-digested with *Bbv*CI and *Blp*I, the 28.5 kb fragment was end-filled with T4 DNA polymerase (Promega UK Ltd., Southampton, UK) and religated with T4 DNA ligase (Promega, Madison, USA). In a second round, the remaining cosmid was double-digested (*Afl*II/*Sna*BI), end-filled and religated to yield a 25.4 kb cosmid containing the entire locus and intergenic regions prior and after the *lat-1* coding region (pTL2).

Transgenes generated by recombineering

For various constructs (*lat-1p::gfp (pTL13), lat-1(1-581)::gfp (pTL20), lat-2::gfp (pTL21), lat-1::gfp (pSP5), lat-1(ΔRBL) (pSP8), lat-1(ΔRBL 1-581)::gfp (pSP9)*) we employed the recombineering toolkit developed by Copeland, Jenkins and coworkers and modified accompanying protocols to construct latrophilin transgenes using cosmids, PCR-ampfilied targeting cassettes, and positive antibiotic selection.

For *lat-1* constructs the cosmid pTL2 was modified with recombineering to accomodate various transgene designs as follows. Electrocompetent *E. coli* SW102 (Warming, 2005) were transformed with the target cosmid, ampicillin-resistant clones were bulked up overnight at 32 °C, the recombinogenic prophage λ in the bacterial culture was induced by heat-shock at 42 °C for 15 min, instantly cooled down in an ice/water slurry, made electrocompetent again using standard protocols and stored in 50 μl aliquots at -80 °C. Target cassettes for recombineering were produced by PCR-amplification of standard antibiotic selection cassettes from different template plasmids using 90 bp primers (Sigma Aldrich, MWG); each primer contained 5' a 60 bp homology region to the targeting site in the cosmid, and 3' a 30 bp homology to the PCR template. PCR products were *Dpn*I-digested and gel-purified. An aliquot of target cosmid-containing, recombination-induced *E. coli* was electroporated with 1 μl targeting DNA (50-100 ng/μl), immediately suspended in 1 ml pre-warmed SOC, transferred to a 15 ml Falcon tube and incubated for 1 hr on a shaker at 32 °C. 50-100 μl of the bacterial culture where then plated on LB agar plates set up for double antibiotic selection for both the cosmid (*amp⁺*) and the targeting cassette (*kan⁺* or *cam⁺*) resistencies. Plates were incubated at 32 °C overnight and successful recombinant colonies picked the next day, bulked up overnight at 32 °C and verified by restriction analyses and sequencing.

pTL13/pTL19: Cosmids pTL13 (*lat-1p::gfp*) and pTL19 (*lat-1(1-493)::gfp*) were engineered by in-frame-targeting a PCR-amplified *gfp::kan* fragment from pPolycistronic (Coates and de Bono, 2002) to appropriate sites within the genomic *lat-1* locus on pTL2.

pSP8: Construct pSP8 (*lat-1⁴³⁷⁻¹³⁶*) was generated in two steps by replacing exon 2 in pTL2 with a *FRT-neo-FRT*-cassette amplified from pIGCN21 using recombineering (Lee, 2001) and co-selection for *amp+/kan+*. The cosmid product containing the *FRT-neo-FRT* insert was electroporated in *E. coli* SW105 (Warming, 2005), in which the site-specific recombinase Flpe was induced with 10 % L(+)-arabinose prior to the transformation. Flpe catalyzed the *FRT-neo-FRT* cassette removal from the cosmid; to verify Flpe-mediated excision efficiency the bacterial culture was split, plated separately on *amp+* and *kan+* LB agar plates, and incubated at 32 °C overnight. Colonies were grown on *amp+* plates, colony numbers on control *kan+* plates were 3 orders of magnitude lower. A few colonies from *amp+* plates were picked, bulked up, and the successful excision was confirmed with restriction digests. In a second step, alternative exons 3a and b on the *Δexon2* cosmid were replaced *en bloc* with a *neo* targeting cassette flanked by *Not*I sites via recombineering and co-selection for *amp+/kan+*. The cassette from the resulting vector was removed by a *Not*I digest and the remaining cosmid recircularized yielding pSP8.

pSP9: Construct pSP9 (*lat-1(1-581)⁴³⁷⁻¹³⁶::gfp*) was produced by releasing a 3.9 kb *Bam*HI-fragment from pTL20 (*lat-1(1-581)::gfp*; not shown) containing the same *gfp::kan* cassette as described for pTL13/pTL19 fused to the genomic sequence coding for the first intracellular loop of *lat-1* and thereby truncating the C-terminal portion of the receptor. The pTL20 fragment was gel-purified and used as a targeting cassette on pSP8. pSP8 was transformed into SW102 beforehand, bacteria were made recombination-competent, recombinant clones were produced and verified following the above protocol.

pSP5: Cosmid pSP5 (*lat-1(1-650)::gfp::lat-1(651-1014)*) was produced by inserting a *gfp* cassette with 5xAla linkers on either side in frame in the second intracellular loop of LAT-1 between D650 and P651. In detail this was achieved by generating an intermediate plasmid (pTL29; not shown); a *FRT-neo-FRT* cassette was inserted into the intronic region between exon 5 and 6 of pTL2 and the entire *exon 5-FRT-neo-FRT-exon 6* segment was retrieved into an outward-PCR-amplified chloramphenicol resistant plasmid backbone with primer-inserted homology arms matching exons 5

and 6; pTL29 was co-selected for *kan+* and *cam+*. pTL29 was again outward-amplified with primers generating a blunt cut between the codons for amino acids 650 and 651; a *gfp* cassette was amplified from pPolycistronic with phosphorylated primers inserting the codons for five alanine residues on either ends of the *gfp* cassette. Both fragments were gel-purified and ligated. The resulting plasmid was linearised with *Acl*I and electroporated into *E. coli* SW105 containing pTL2 to target *exon 5-FRT-neo-FRT-exon 6::gfp* to its homologous sites in pTL2 and clones were co-selected for *amp+* and *kan+*. The *FRT-neo-FRT* cassette was removed in a final round of Flp-mediated excision in SW105 as described above.

pSP36: To yield construct pSP36 (*lat-1(1-581)$^{\Delta483-542}$::gfp*) a genomic deletion targeting cassette lacking cosmid sequence corresponding to aa483-542 for *lat-1* was constructed by amplifying two separate fragments from pTL20; the 3'-fragment also included the *gfp::kan* cassette of pTL20. Each of the two PCR reactions contained a phosphorylated primer (reverse primer for fragment 1; forward primer for fragment 2) subsequently allowing for the efficient ligation of both fragments with T4 ligase (NEB). The resulting DNA fusion product was re-amplified over the entire length and targeted to the appropriate region in pTL2 as described above.

Recombinant protein expression

C. elegans LAT-1A RBL domain sequence (residues T32-T139) was amplified from EST clone *yk1336f09*, tagged for secretion using the α-factor signal propeptide sequence and cloned in a modified pPICZα vector (Invitrogen). Residue substitutions were constructed using a PCR-based method. Expression and purification was carried out as previously described (Vakonakis et al., 2008). In short, constructs were electroporated in *P. pastoris* strain X-33. The secreted and concentrated protein was dialyzed against a 10 mM sodium phosphate pH 7.0 buffer and further purified by anion exchange chromatography (Q-sepharose, GE Biosciences), followed by dialysis against the final NMR buffer and concentration using Amicon spin-columns (Millipore).

SUPPLEMENTAL REFERENCES

Bischoff, M., and Schnabel, R. (2006). A posterior centre establishes and maintains polarity of the Caenorhabditis elegans embryo by a Wnt-dependent relay mechanism. PLoS Biol *4*, e396.

Coates, J.C., de Bono, M. (2002). Antagonistic pathways in neurons exposed to body fluid regulate social feeding in Caenorhabditis elegans. Nature *419*, 925-9.

Lee EC, Yu D, Martinez de Velasco J, Tessarollo L, Swing DA, Court DL, Jenkins NA, Copeland NG. (2001). A highly efficient Escherichia coli-based chromosome engineering system adapted for recombinogenic targeting and subcloning of BAC DNA. Genomics *73*, 56-65.

Ozeki, Y., Matsui, T., Nitta, K., Kawauchi, H., Takayanagi, Y., and Titani, K. (1991a). Purification and characterization of beta-galactoside binding lectin from frog (Rana catesbeiana) eggs. Biochem Biophys Res Commun *178*, 407-413.

Ozeki, Y., Matsui, T., Suzuki, M., and Titani, K. (1991b). Amino acid sequence and molecular characterization of a D-galactoside-specific lectin purified from sea urchin (Anthocidaris crassispina) eggs. Biochemistry *30*, 2391-2394.

Steinel, M.C., and Whitington, P.M. (2009). The atypical cadherin Flamingo is required for sensory axon advance beyond intermediate target cells. Dev Biol *327*, 447-457.

Vakonakis, I., Langenhan, T., Prömel, S., Russ, A., and Campbell, I.D. (2008). Solution structure and sugar-binding mechanism of mouse latrophilin-1 RBL: a 7TM receptor-attached lectin-like domain. Structure *16*, 944-953.

Volynski K.E., Silva J.P., Lelianova V.G., Atiqur Rahman M., Hopkins C., Ushkaryov Y.A. (2004). Latrophilin fragments behave as independent proteins that associate and signal on binding of LTX(N4C). EMBO J *23*, 4423-33.

Warming, S., Costantino, N.,Court, D.L., Jenkins, N.A., Copeland, N.G. (2005). Simple and highly efficient BAC recombineering using galK selection. Nucleic Acids Res *33*, e36.